

Smad3 Is Required for Normal Follicular Follicle-Stimulating Hormone Responsiveness in the Mouse¹

Xiaoyan Gong and Elizabeth A. McGee²

Department of Obstetrics and Gynecology, Virginia Commonwealth University, Richmond, Virginia

ABSTRACT

Follicle-stimulating hormone (FSH) is the major regulator of folliculogenesis, but other factors modulate its action, including members of the transforming growth factor (TGF) beta family. The intersection of signal transduction pathways that integrate the follicular response to FSH remains to be elucidated. Herein, we investigated the role of *Smad3*, a critical molecule mediating the intracellular TGFbeta family proteins, in follicle development and the expression of FSH receptors. We found that gonadotropin stimulation could not induce normal ovulation in *Smad3*-deficient mice. Moreover, FSH could not stimulate early follicle growth in *Smad3*-deficient mice in in vivo or in vitro systems. Cultured granulosa cells from *Smad3*-deficient animals had reduced cell division rates following FSH treatment compared with granulosa cells derived from the ovaries of wild-type (WT) mice. Whole ovaries and isolated granulosa cells from *Smad3*-deficient animals had lower basal expression of FSH receptor (*Fshr*), aromatase (*Cyp19a1*), and cyclin D2 (*Ccnd2*) mRNA compared with WT mice. Follicle-stimulating hormone treatment of granulosa cells from WT ovaries upregulated *Fshr*, *Cyp19a1*, and *Ccnd2* expression. However, FSH did not increase these mRNAs in *Smad3*-deficient granulosa cells. When *Smad3* was introduced into *Smad3*-deficient granulosa cells with adenovirus vectors, FSH responsiveness was restored, and FSH was able to upregulate *Fshr* expression. Furthermore, SMAD3 interacts with a palindromic SMAD binding element in the *Fshr* promoter, and TGFB can activate promoter constructs containing this element. Collectively, these observations establish an essential role for *Smad3* in regulating the response of ovarian follicles to FSH.

fertility, follicle-stimulating hormone receptor, folliculogenesis, *Fshr*, mechanisms of hormone action, ovary, *Smad3*

INTRODUCTION

Fertility in mammalian females is dependent on the growth of follicles, structural units consisting of an oocyte, granulosa cells, and theca cells with an extracellular matrix separating the cell layers. Follicles develop through stages beginning with primordial follicles, containing a small oocyte surrounded by a layer of fibroblast-like granulosa cells, through primary, preantral, antral, to the preovulatory or Graafian stage,

containing a fully grown oocyte and multiple layers of granulosa cells. After ovulation and release of the oocyte, the remaining cells participate in the formation of a corpus luteum, which sustains pregnancy in a fertile cycle. Significant disruption occurring at any of the stages of follicle development impairs fertility and alters ovarian hormone production [1].

The regulation of follicle growth has been studied for many years; however, regulation of the early stages of folliculogenesis has lagged behind the study of antral and preovulatory follicles. Early follicles express follicle-stimulating hormone (FSH) receptors and can respond to FSH treatment with increased follicle growth and development [1, 2]. Early follicles also respond to other growth factors that augment or modify the effects of FSH on granulosa cells [3]. Many members of the transforming growth factor (TGF) β superfamily are thought to have important roles in several stages of folliculogenesis [1, 4]. Activin and TGF β have both been reported to be involved in FSH receptor upregulation in granulosa cells [5, 6]. Various effects of TGF β family members have also been demonstrated in whole-follicle studies [7–10].

A family of closely related proteins known as SMADs mediates signal transduction of the TGF β family of growth factors [11]. They are divided into three functional groups with mediating, receptor-activated, and inhibitory roles. The bone morphogenic protein subgroup of the TGF β family largely signals via SMAD1, SMAD5, and SMAD8. The TGF β and activin subgroups signal via SMAD2 and SMAD3.

SMAD2 and SMAD3 are both highly expressed in follicles from the primordial stage to the late preantral and early antral stages. Expression decreases in large antral and preovulatory follicles. Although a low level of SMAD2 expression returns to the corpus luteum, SMAD3 is not expressed in the corpus luteum [12]. Female mice deficient in SMAD3 have impaired fertility [13, 14], but the cause of the infertility has not been specifically determined. These mice have a normal follicle endowment of primordial follicles but have reduced numbers of small growing follicles [13]. There are no litters from females, and at age 90 days they do not ovulate in response to exogenous gonadotropins [14]. Markers for cell division are normal at age 18 days but are reduced by age 30 days [13, 14]. However, these studies did not explore the dynamics of gonadotropin treatment on follicle growth and development.

In this study, we evaluated the role of *Smad3* in FSH-stimulated follicle growth, granulosa cell division, and FSH receptor expression. Preantral follicles have a markedly reduced growth rate in response to FSH stimulation in the absence of *Smad3*. Granulosa cells also have reduced cell division and *Cyp19a1* expression. There is impaired expression of *Fshr* in the absence of *Smad3* that can be restored with *Smad3* expression. SMAD3 associates with a SMAD binding element (SBE) in the *Fshr* promoter, and TGFB treatment activates a promoter construct containing this site. Thus, *Smad3* is required for the optimal regulation of FSH receptor expression during folliculogenesis in the mouse.

¹Supported by R01 HD045700.

²Correspondence: Elizabeth A. McGee, Department of Obstetrics and Gynecology, Virginia Commonwealth University, P.O. Box 980034, Richmond, VA 23298. FAX: 804 828 0573; e-mail: eamcgee@vcu.edu

Received: 22 April 2008.

First decision: 24 May 2008.

Accepted: 15 May 2009.

© 2009 by the Society for the Study of Reproduction, Inc.

This is an Open Access article, freely available through *Biology of Reproduction's* Authors' Choice option.

eISSN: 1259-7268 <http://www.biolreprod.org>

ISSN: 0006-3363

MATERIALS AND METHODS

Animals

All animal experiments were performed in accord with National Institutes of Health guidelines and with institutional approval. *Smad3*-deficient mice (*Smad3*^{-/-}) were generated by disrupting exon 8 of the *Smad3* gene by homologous recombination, which is described in detail elsewhere [15]. These animals were created on a C57BL6/SVEV129 hybrid background and do not express SMAD3 protein [16, 17]. Animals were housed under standard conditions for breeding colonies under 12L:12D cycles and with standard rodent chow continuously available. Offspring were genotyped as previously described [13, 15]. Ovulation induction was carried out in the standard fashion [18]. Equine chorionic gonadotropin (10 IU; Sigma-Aldrich, St. Louis, MO) was administered s.c., followed 48 h later by human chorionic gonadotropin (10 IU; Sigma-Aldrich). Approximately 22 h later, animals were euthanized, and fallopian tubes and uteri were dissected and searched for ovulated oocytes as previously described [18].

Follicle Culture

Ovaries were dissected from 18-day-old wild-type (WT) and knockout (KO) (*Smad3* deficient) mice and placed into embryo culture dishes in warmed Leibovitz L-15 medium as previously described [8, 19, 20]. Preantral follicles of 130–140 μ m in diameter were dissected microscopically using fine needles. Follicles were cultured individually in 96-well dishes in α -modified Eagle medium (Invitrogen, Carlsbad, CA) supplemented with ITS + Culture Supplement (contains 1.0 mg/ml insulin, 0.55 mg/ml human transferrin, 0.5 μ g/ml sodium selenite, 50 mg/ml bovine serum albumin (BSA), and 470 μ g/ml linoleic acid; Sigma-Aldrich), 100 nM 8-bromo-cGMP, and Pen/Strep (100 U/ml penicillin and 100 μ g/ml streptomycin; Invitrogen) at 37°C in a humid atmosphere containing 5% CO₂. Follicles were obtained from two different WT mice and two different KO mice for each experiment. At least 20 follicles were included in each treatment group.

Granulosa Cell Culture

For primary granulosa cell culture, ovaries from 25- to 30-day-old female mice were removed and dissected free of connective tissue. Ovaries were incubated in McCoy 5A (Sigma-Aldrich) medium containing 1.8 mM ethyleneglycoltetracetic acid and 26 mM sodium bicarbonate at 37°C for 10 min, and then in McCoy 5A with 0.5 M sucrose at 37°C for 5 min as previously described [21]. Puncture of antral follicles was performed under microscopic visualization. The cells were pelleted and resuspended and were counted using a hemocytometer. Viability was determined by trypan blue staining. Cells were cultured in McCoy 5A medium containing 10% fetal bovine serum (FBS) and Pen/Strep at 37°C in a humid atmosphere containing 5% CO₂. After 24 h, the medium was changed to serum-free McCoy 5A medium containing 0.1% BSA and 10 μ l/ml ITS + Culture Supplement for 24 h before performing the experiments.

Histology and Immunofluorescence Staining

For histological examination of tissue sections, ovaries were fixed in Bouin reagent or 4% paraformaldehyde (Sigma-Aldrich) overnight at 4°C and then embedded in paraffin. Six-micrometer sections were cut and stained with hematoxylin-eosin.

Granulosa cells were grown in glass chamber slides. After treatments, cells were washed with PBS three times, fixed in 4% paraformaldehyde for 10 min, and then preincubated with 10% goat serum/PBS for 20 min. Cells were incubated with rabbit polyclonal antibody against SMAD3 (1:100 dilution in PBS; Zymed Laboratories, South San Francisco, CA) for 2 h at room temperature. Slides were washed with cold PBS and incubated with biotinylated anti-rabbit IgG antibody (1:200 in PBS; Vector Laboratories, Burlingame, CA) for 30 min at room temperature. Slides were washed and incubated with Texas Red Avidin D (6 μ g/ml in PBS; Vector Laboratories) for 10 min and were mounted with Vectashield mounting medium containing 4',6'-diamidino-2-phenylindole (Vector Laboratories).

For proliferation studies, cells were labeled with bromodeoxyuridine (BrdU) at 37°C for 2 h, fixed with 70% ethanol, and stained according to the manufacturer's instructions using the BrdU staining kit from Invitrogen. One hundred cells from each well were counted and scored as stained or not stained by a counter unaware of the treatment group or source of cells.

For apoptosis studies, cells were fixed in 4% paraformaldehyde and permeabilized by 0.2% Triton X-100. Cells were then analyzed using a DeadEnd colorimetric TUNEL system (Promega, Madison, WI) according to the manufacturer's protocol. The percentage of dark-staining apoptotic nuclei

was determined by counting 1000 cells on four different coverslips per group and scoring each cell as stained or not stained. Groups were unknown to the person counting the cells.

RNA Isolation and Real-Time PCR Analysis

RNA was isolated from ovaries or granulosa cells using TRIzol reagent (Invitrogen) following the manufacturer's protocol. The RT cDNA synthesis reactions were performed using oligo (dT) M-MLV RT (Ambion, Austin, TX) with 0.5–1.5 μ g of total RNA under the conditions described by the manufacturer.

For real-time PCR, the TaqMan assay system was used (Applied Biosystems, Foster City, CA) with specific probes for mouse FSH receptor (*Fshr* [catalog number Mm00442819]), TATA (*Tbp* [Mm00446973]), aromatase (*Cyp19a1* [Mm00484049]), and cyclin D2 (*Ccnd2* [Mm00438071]). Probes were labeled at the 5' end with FAM (6-carboxy-fluorescein) reporter dye. The real-time PCR reaction was completed on an ABI 7500 Thermocycler (Applied Biosystems) with 2 min at 50°C (AmpErase UNG activation), 10 min at 95°C (AmpliTaQ Gold DNA polymerase activation), and 40 cycles each with 15 sec at 95°C (melting) and 1 min at 60°C (annealing/extension). The C_T value was determined for each reaction (run in duplicate) using Sequence Detection Software version 1.7a (Applied Biosystems), and quantification was completed using the $\Delta\Delta C_T$ method [22]. *Tbp* is a well-characterized housekeeping gene [23] that is expressed at low levels, similar in magnitude to *Fshr*.

Chromatin Immunoprecipitation

The chromatin immunoprecipitation (ChIP) assay was performed using an EZ ChIP kit (Upstate, Temecula, CA). Wild-type mouse granulosa cells were cultured for 48 h with FSH (1 IU/ml). Cells were treated with 1% formaldehyde (Sigma-Aldrich) at 37°C for 10 min to cross-link proteins to DNA. The reaction was stopped with glycine, and the cells were lysed. Samples were then sonicated on ice for 30 min in 30-sec bursts each at a maximal input using Bioruptor UCD-200TM-EX (Diagenode, Sparta, NJ) and then centrifuged for 10 min at 12000 $\times g$ at 4°C. Chromatin was precleared with salmon sperm DNA/protein G agarose for 1 h at 4°C, and 1% of this solution was saved for use as input chromatin. Samples were incubated overnight with a ChIP-grade SMAD3 antibody (Abcam, Cambridge, MA) or with normal rabbit IgG (negative control; Santa Cruz Biotechnology, Santa Cruz, CA). Samples were then incubated, pelleted, and washed as per the manufacturer's instructions. Immunocomplexes were eluted from the agarose beads. Input and immunoprecipitated chromatin was incubated with 200 mM NaCl at 65°C overnight to reverse DNA-protein cross-links. DNA was purified as per the manufacturer's instructions and analyzed by PCR using specific primers for the SBE site (forward primer 5'-CAGTGTGTAACCATTTTCAGGAGA-3' and reverse primer 5'-TCCACCCAGAGTCTATGAACACTA-3'); the PCR product is 135 base pair [bp] in length) and the non-SBE site (forward primer 5'-AGGTCTTGAAGGATAAGACAGGTG-3' and reverse primer 5'-ACA CACTGTCCGGATAAGAGAGAT-3'; the PCR product is 198 bp in length).

FSH Receptor Promoter-Luciferase Reporter Constructs

Mouse *Fshr* promoter-luciferase reporter constructs were created using the pGL-3 basic vector system (Promega). A genomic DNA fragment containing the 1.55-kilobase *Fshr* 5'-flanking region was amplified by PCR using WT female mouse genomic DNA with forward primer 5'-GGTACCTTG CAACTTCCACCATG-3' (*KpnI*) and reverse primer 5'-CTCGAGGCT TATTTATCCATCCAC-3' (*XhoI*). The PCR product was cloned into PCR2.1-TOPO TA vector (Invitrogen). The -1035/+536 promoter fragment was then subcloned into the *KpnI/XhoI* sites of the pGL-3 basic vector. A truncated *Fshr* promoter construct (FRP truncated) was also generated. The fragment was amplified with forward primer 5'GGTACCGACTATGG TTTATAAC-3' (*KpnI*) and reverse primer 5'-CTCGAGGCTTATTTATCC ATCCAC-3' (*XhoI*). An *Fshr* promoter construct with an SBE deletion was generated using the QuickChange site-directed mutagenesis kit (Stratagene, La Jolla, CA) according to the manufacturer's protocol. The sequence "TAGAC" was deleted from the SBE "CTAGAC" sequence. All *Fshr* promoter constructs were verified by sequencing.

Cell Culture, Transient Transfection, and Luciferase Assays

The luciferase reporter constructs were transfected into a well-characterized granulosa cell line [24, 25] that was kindly provided by Dr. Robert Burghardt, Texas A&M University, College Station, TX [26]. Cells were cultured in Dulbecco modified Eagle medium (DMEM)/F-12 with 5% FBS, 100 U/ml

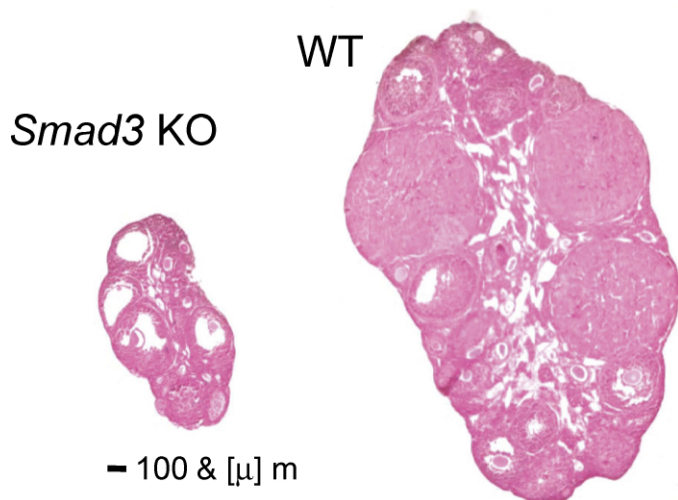


FIG. 1. Representative sections of WT and *Smad3*-deficient (KO) ovaries from young adult (age 48 days) sibling mice. Bar = 100 μ m.

penicillin, and 100 μ g/ml streptomycin (all from Invitrogen) and were seeded at a density of 8×10^4 cells/well in 12-well plates 1 day before transfection, which was performed with Eugene 6 (Roche Diagnostics, Indianapolis, IN) following the manufacturer's protocol. Cells were transfected with 0.5 μ g of indicated plasmid DNA and 10 ng of internal control Renilla DNA. Cells were serum starved for 8 h before incubating with or without 1 ng/ml of TGF β -1 (R&D Systems, Minneapolis, MN) for 16 h. The Dual-Luciferase Reporter Assay System (Promega) was used following the manufacturer's protocol. Luciferase activity was normalized relative to the activity of pGl-3 basic vector.

Adenoviral Infection of Primary Granulosa Cells

Adenoviruses containing *Smad3* (Ad*Smad3*) and *Gfp* (Ad*GFP*) were constructed and prepared using the AdMax system (Micobix, Toronto, ON, Canada) according to the manufacturer's directions with assistance from Dr. Anthony Zeleznik (Pittsburgh, PA). This construct is described in detail elsewhere [27]. Initially, 293 cells were transfected with the adenoviral vector DNA and maintained in DMEM containing 3% FBS at 37°C in 5% CO₂ for 10 days or until plaques exhibiting viral cytopathic effects were identified. A second large-scale amplification was carried out, and purification was performed using CsCl density gradient ultracentrifugation. The optical density of the samples at 260 nm was used to calculate virus content using the relationship of 1.1×10^{12} virus particles/ml per A₂₆₀ unit. Expression of SMAD3 protein after adenovirus infection of granulosa cells was confirmed by both Western analysis and immunohistochemistry. Transfection efficiency routinely exceeded 90% [28].

Smad3-deficient granulosa cells were seeded into 48-well tissue culture plates or eight-well glass chamber slides and were allowed to attach for 24–48 h. Before infection, medium and unattached cells were removed, and granulosa cell monolayers were exposed to recombinant adenovirus vector Ad*Smad3* (multiplicity of infection [MOI] = 200) in McCoy 5A medium for 2 h. Medium was then replaced with fresh serum-free medium (McCoy 5A medium containing 0.1% BSA and 10 μ l/ml ITS + Culture supplement) for 24 h before experiments.

Data Analysis

Experiments were repeated at least three times, and results were reported as the mean \pm SEM. Data were subjected to ANOVA and post hoc testing with Tukey honestly significant difference test when more than two groups were compared. Student *t*-test was used for single comparisons. Statistical significance was accepted at $P < 0.05$.

RESULTS

The Ovaries of *Smad3*-Deficient Mice Did Not Respond Normally to Endogenous or Exogenous Gonadotropins

Observations of female mice (WT and heterozygous and homozygous for the mutant *Smad3* allele) were made on a

TABLE 1. Growth of preantral follicles in culture.

Genotype	FSH treatment ^a	Starting diameter (μ m \pm SD)	Ending diameter (μ m \pm SD)	Difference ^b
WT	–	132.0 \pm 8.3	133.0 \pm 11.7	NS
WT	+	131.0 \pm 7.3	196.0 \pm 14.9	$P < 0.05$
KO	–	139.0 \pm 11.6	141.0 \pm 15.0	NS
KO	+	140.2 \pm 10.6	151.0 \pm 13.3	NS

^a –, Without treatment; +, with treatment.

^b NS, not significant.

daily basis. Vaginal opening occurred at a similar age in all three genotypes. However, following vaginal opening, *Smad3*-deficient females seldom had normal estrous cycles. In a group of six *Smad3* KO and six WT sister pairs, daily vaginal smears revealed that over a 4-wk period the six WT females had 40 estrous cycles, while there was only one normal estrous cycle in the KO group over the same observation time.

The capacity of *Smad3*-deficient mice to ovulate in response to exogenously administered gonadotropins was evaluated at age 56–60 days. Wild-type females ($n = 6$) ovulated 12–16 eggs when treated with exogenous gonadotropins. Most homozygous mutant mice ($n = 6$) did not ovulate, except for one animal that ovulated one egg. We maintained histological or morphological observations of all ovaries harvested from the colony, and ovaries from untreated *Smad3*-deficient mice only rarely contained corpora lutea and never past age 60 days. This is similar to a previous study [14] in which no ovulations were observed in *Smad3*-deficient animals at age 90 days. Figure 1 shows representative ovary sections from both a *Smad3*-deficient and a WT sister pair at age 48 days.

Because of diminished cyclicality and poor ovulatory response to exogenous gonadotropins in the *Smad3*-deficient ovaries, we next determined the ability of early preantral follicles to respond to FSH treatment. Table 1 summarizes the growth of individually isolated preantral follicles in four experimental groups that included 20–30 follicles in each group. Follicles of 130–140 μ m in diameter were mechanically dissected from whole ovaries from WT and *Smad3*-deficient animals and were individually cultured in 96-well plates. In the absence of FSH, neither WT nor *Smad3*-deficient follicles increased in diameter. As expected, follicles from WT ovaries grew in response to FSH treatment. A 60- μ m increase over 3 days of culture with FSH is consistent with what we and others have shown previously [8, 29]. However, the follicles from *Smad3*-deficient ovaries did not increase in diameter in response to treatment with FSH. Thus, *Smad3*-deficient preantral follicles exhibited a limited response to FSH stimulation *in vitro*.

We next determined whether preantral follicles from *Smad3*-deficient mice respond to FSH treatment *in vivo*. In these studies, FSH was administered every 12 h from age 15 days to age 19 days. The average weight of untreated ovaries at age 19 days is 0.42 ± 0.04 mg ($n = 6$). The weight of the FSH-stimulated WT ovaries at age 19 days increased three-fold to 1.40 ± 0.25 mg ($n = 8$) ($P < 0.05$ compared with untreated control). In contrast, ovarian weight did not increase in the *Smad3*-deficient animals treated with FSH (0.37 ± 0.10 mg for treated ovaries [$n = 4$] versus 0.25 ± 0.05 mg for untreated ovaries [$n = 4$]).

To determine the effect that FSH treatment had on cell division within follicles, we also treated the animals with the marker BrdU 1 h before termination of the experiment [30]. Cells that are in the synthesis phase of cell division stain brown. Figure 2, A and B, shows BrdU-stained sections of ovaries from these experiments, whereas Figure 2, D and D,

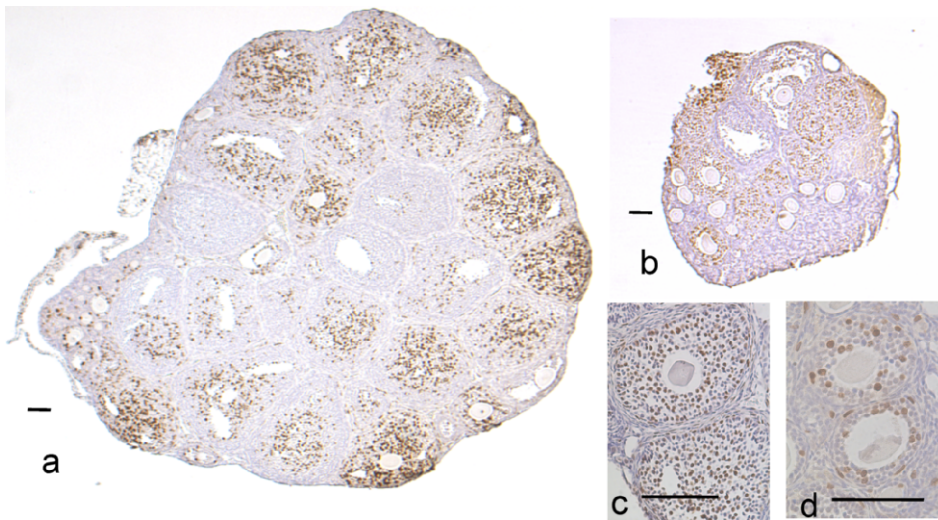


FIG. 2. Bromodeoxyuridine-stained ovaries from immature mice treated with FSH in vivo from age 15 days to age 19 days. **A)** Wild-type ovary section stained for BrdU (brown). **B)** Section of identically treated *Smad3*-deficient (KO) ovary. Images were reproduced identically, so the size differential reflects the difference in size of the ovaries. Also shown are higher magnifications of multilaminar preantral follicles from WT ovary (**C**) and KO ovary (**D**). Bar = 100 μ m.

shows higher-magnification representative staining patterns of follicles from each group. The ovaries from the FSH-treated WT animals showed robust follicle growth and had large preantral follicles containing multiple layers of granulosa cells with readily apparent BrdU staining (Fig. 2C). In contrast, the *Smad3*-deficient ovaries had minimal follicle growth response to FSH treatment. The follicles contained few layers of granulosa cells and only sporadically stained for BrdU, consistent with reduced granulosa growth response (Fig. 2D).

The proliferation index was determined for small preantral follicles with 3–5 layers of granulosa cells (and follicle diameters between 130 and 150 μ m) from the ovaries from these experiments. Twenty-five to 30 follicles that were sectioned through the oocyte were identified in sections from four ovaries from each group. More than 100 total follicles were assessed each in WT and KO ovaries. All of the granulosa cells in the follicle cross-section were counted, and the number of cells that stained for BrdU was noted. The percentage of stained cells reflects the proliferation index of the follicle. The WT preantral follicles had a proliferation index of $23.3\% \pm 2.9\%$, whereas the *Smad3*-deficient follicles had a proliferation index of only $3.5\% \pm 0.6\%$ ($P < 0.05$). Thus, the number of dividing cells in similarly sized follicles was reduced in *Smad3*-deficient ovaries treated with FSH compared with WT ovaries.

Granulosa Cells from Ovaries of *Smad3*-Deficient Mice Showed Diminished Mitotic Activity in Response to FSH Treatment In Vitro

To analyze the FSH effect on granulosa cell division more closely, we performed granulosa cell culture with cells isolated from the ovaries of mice aged 21–25 days (Fig. 3A). Cells were grown in chamber slides as described in *Materials and Methods*. Cells from either WT or *Smad3*-deficient mice were pooled from 2 to 4 animals per experiment and grown in the presence or absence of FSH (1 IU/ml) for 24 h. At the end of the experiment, the cells were incubated with BrdU to mark the cells in the synthesis phase of cell division. Positively stained cells were counted from at least three wells per group, and the experiment was repeated three times. As shown in Figure 3A, there was a low baseline rate of cell division in both WT and *Smad3*-deficient cells. However, FSH stimulated cell division in WT cells to a much greater extent than that in *Smad3*-deficient cells ($P < 0.05$). Thus, cultured granulosa cells were less responsive to FSH treatment in the absence of *Smad3*.

Cells were also analyzed for apoptosis at the end of the experiments using a TUNEL assay to label free DNA ends. Figure 3B shows the low but consistent rate of apoptosis in all the experimental groups of cells. Both *Smad3*-deficient and WT cells survive well in this culture system.

Expression of Key Genes Involved in Granulosa Cell Function Was Reduced in the Ovaries and Granulosa Cells of *Smad3*-Deficient Mice

We next evaluated the expression of *Fshr*, *Ccnd2*, and *Cyp19a1* mRNAs as indices of the response to FSH in ovaries and granulosa cells of WT and *Smad3*-deficient mice. *Ccnd2* was used as a marker of cell division and *Cyp19a1* as a marker of granulosa cell differentiation [1]. In whole ovaries (Fig. 4A), endogenous expression of all of these mRNAs was markedly reduced in the *Smad3*-deficient ovaries as determined by quantitative real-time PCR. In granulosa cells isolated from *Smad3*-deficient ovaries (Fig. 4B), the expression of *Fshr*, *Cyp19a1*, and *Ccnd2* mRNAs was reduced in granulosa cells compared with WT matched controls.

To determine the effect of FSH treatment on gene expression in granulosa cells in vitro, we cultured granulosa cells from both from WT and *Smad3*-deficient mice with or

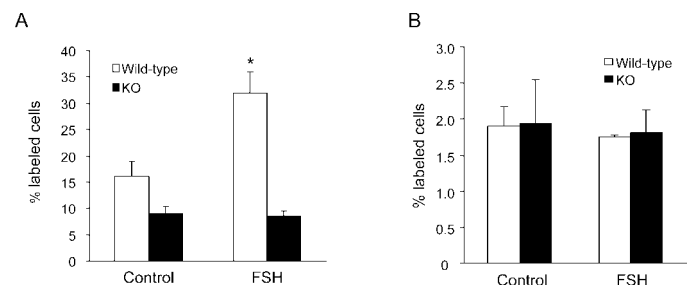
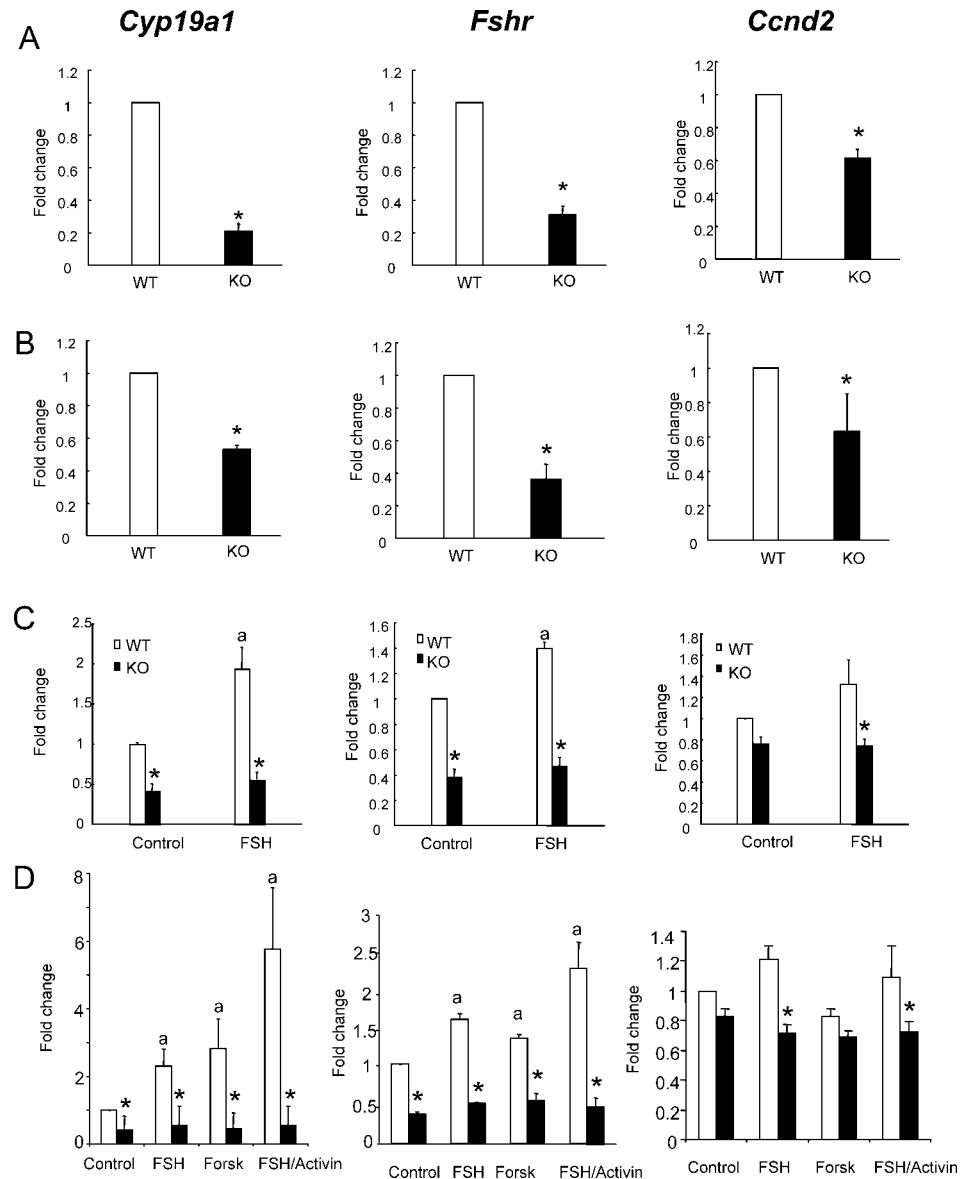


FIG. 3. Response of cultured granulosa cells to FSH treatment. Cells isolated from WT and KO ovaries were grown as described in *Materials and Methods*. **A)** After FSH treatment (1 IU/ml), cells were incubated with BrdU, fixed, and stained. Data are presented as the mean \pm SEM number of stained cells for four experiments. Follicle-stimulating hormone treatment doubled the percentage of BrdU-stained cells in the WT cells ($P < 0.05$), but the KO cells had no change in the percentage of BrdU-stained cells. *, Different from control. **B)** Cells similarly treated but fixed and stained for free DNA ends with a TUNEL assay. Data are presented as the mean \pm SEM number of stained cells for four experiments. The low basal rate of apoptosis is not different between the groups.

FIG. 4. Differential expression and regulation of key genes in ovaries and granulosa cells of WT and KO mice. **A**) Whole-ovary expression of mRNA for *Cyp19a1*, *Fshr*, and *Ccnd2*. **B**) Freshly isolated granulosa cell expression of *Cyp19a1*, *Fshr*, and *Ccnd2* mRNA. **C**) Granulosa cells cultured for 48 h without (control) or with FSH (1 IU/ml). Follicle-stimulating hormone treatment up-regulates expression for *Cyp19a1*, *Fshr*, and *Ccnd2* in cells isolated from WT but not *Smad3* KO mice. **D**) Granulosa cells treated for 48 h with FSH (1 IU/ml), forskolin (Forsk) (10 nM), or FSH in combination with activin A (10 ng/ml) and evaluated for *Cyp19a1*, *Fshr*, and *Ccnd2* expression. Open bars represent WT ovaries or granulosa cells. Black bars represent *Smad3* KO ovaries or granulosa cells. a, Different from control group ($P < 0.05$). *, Different from WT of same treatment ($P < 0.05$). Experiments were repeated three times.



without FSH (1 IU/ml) for 24 h (Fig. 4C). The cells were then lysed, and mRNA was isolated for quantitative real-time PCR determination of expression of *Fshr*, *Cyp19a1*, and *Ccnd2* mRNAs. In the WT cells, FSH treatment stimulated increased expression of *Cyp19a1*, *Fshr*, and *Ccnd2* [1]. However, the expression of *Fshr*, *Cyp19a1*, and *Ccnd2* mRNAs was not increased in the granulosa cells from the KO mice ($P > 0.05$). Thus, FSH was not able to upregulate the expression of its own receptor in the absence of *Smad3*. Furthermore, the expression of downstream markers of cell division and differentiation was also impaired in the cells in the absence of *Smad3*, consistent with diminished FSH receptor function.

Granulosa cells from WT and *Smad3*-deficient mice were also treated with forskolin, an activator of adenylate cyclase (Fig. 4D). Forskolin treatment had the same effect as FSH treatment on *Fshr* and *Cyp19a1* mRNA expression but did not stimulate *Ccnd2* expression. This is not unexpected given that *Ccnd2* is not thought to be a cAMP-regulated response to FSH receptor activation [31]. Activin augmented the FSH-induced effects in the WT cells but not in the *Smad3*-deficient cells. In

the absence of *Smad3*, FSH, forskolin, and FSH/activin were all unable to upregulate FSH receptor expression.

Restoration of *Smad3* Signaling Corrected the Defects in FSH Responsiveness in Granulosa Cells of *Smad3*-Deficient Mice

To determine if the absence of *Smad3* prevented the upregulation of FSH receptor in *Smad3*-deficient mice, we performed experiments to restore SMAD3 to the *Smad3*-deficient granulosa cells (Fig. 5). Granulosa cells from WT and *Smad3*-deficient mice were infected with adenovirus vectors containing a functional *Smad3* construct or *Gfp* as a control. In the absence of FSH treatment, cells had low basal expression of *Fshr*. However, in the presence of FSH, the WT cells had increased expression of *Fshr*. The *Smad3*-deficient cells did not respond to FSH treatment. However, when functional *Smad3* was added back to the KO cells with the adenovirus, the ability of the granulosa cells to respond to FSH treatment was restored (Fig. 5A). Although SMAD3 was not detected in the uninfected granulosa cells (Fig. 5B, a and b), SMAD3 protein

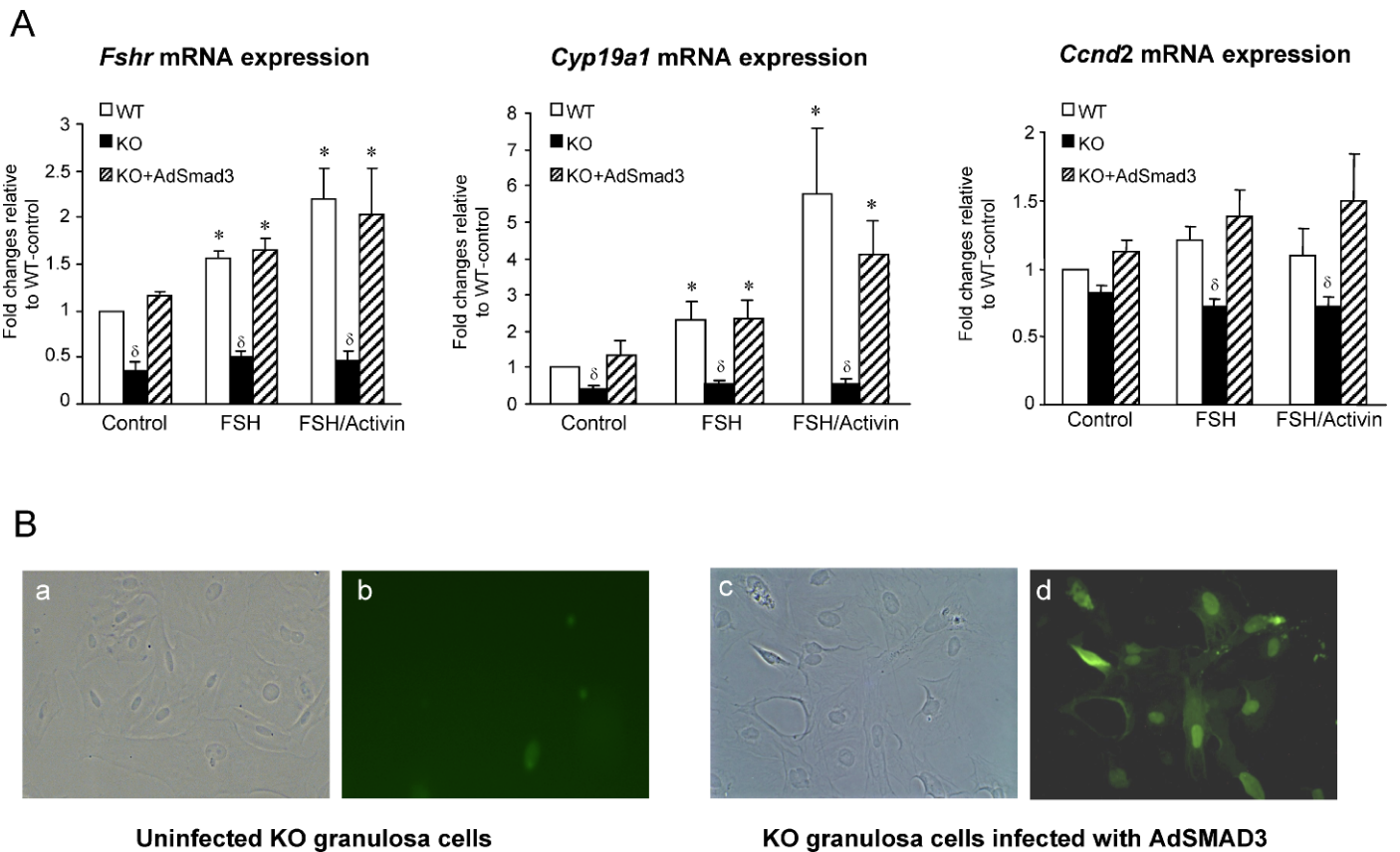


FIG. 5. Restoration of *Smad3* expression restores FSH responsiveness. **A**) Follicle-stimulating hormone receptor expression in granulosa cells from WT and *Smad3* KO mice treated without or with FSH. Cells were infected with adenoviral vectors containing GFP as a control (WT and KO [open and dark bars, respectively]), except for the KO cells that were infected with adenovirus containing *Smad3* (KO + AdSmad3 [hatched bars]). *Smad3* KO cells infected with *Smad3* regained the ability to increase *Fshr* and *Cyp19a1* expression in response to FSH and FSH/activin treatment. *, Different from control treatment group of same cell type ($P < 0.05$). δ , Different from WT cells of the same treatment group ($P < 0.05$). **B**) Uninfected KO cells (a and b) and KO cells after infection with AdSmad3 (c and d) (a and c are phase-contrast images of cells, and b and d represent immunohistochemistry of cells stained for SMAD3 protein). No protein is present in KO cells that are not infected with the adenovirus construct, but SMAD3 nuclear staining (green) is present in most cells after infection with AdSmad3 (original magnification $\times 200$).

was readily detected in cells infected with the *Smad3* vector (Fig. 5B, c and d).

Fshr Promoter Contains a SMAD Responsive-Element

Examination of the 5' untranslated region of the mouse *Fshr* gene sequence revealed a palindromic SBE site [32, 33] –440 bp upstream of the transcription start site (Fig. 6); *Fshr* promoter constructs were generated to analyze the function of this site. Granulosa cells from a spontaneously immortalized cell line [26] were transfected with these constructs and treated with TGF β . Cells transfected with the *Fshr* promoter constructs containing this SBE site (FRP) responded to TGF β treatment but not when the SBE site was deleted (FRP-del-SBE) (Fig. 6A) or mutated (data not shown).

To investigate if SMAD3 binds to the SBE site in the *Fshr* promoter (Fig. 6B), we next performed a ChIP analysis with SMAD3 antibody. Figure 6C shows that SMAD3 binds to the SBE site at –440 bp but not at +406 bp, which contains an AP-1/E-Box site. It has been shown that SMAD3 forms complexes with other transcription factors and binds to some AP-1 sites [34], but our experiment demonstrates that it does not in the *Fshr* promoter. Also, SMAD3 did not bind other AP-1, SF-1, or TGF β sites analyzed in the *Fshr* promoter [35] (data not shown). SMAD3 can specifically bind to the palindromic SBE

site in the *Fshr* promoter region at –440 bp, and the promoter activity was increased with the stimulation of TGF β .

DISCUSSION

We have demonstrated that in the absence of *Smad3* preantral follicles are unable to respond appropriately to FSH stimulation. It was known that there is a delay in the presence of multilayered follicles and antral follicles in the first wave of follicles in the ovaries in *Smad3*-deficient mice [13]. Although follicles can progress to the antral stage, they do not do so in a normal time frame or in conventional numbers. We have shown that there is a delay in the growth of isolated preantral follicles in response to FSH treatment, which may account for this disruption of the normal temporal pace of follicular development in vivo (Table 1). Follicle-stimulating hormone-stimulated cell division in preantral follicles in vivo is also reduced in the absence of *Smad3* (Fig. 2). We have also shown reduced expression of *Fshr* and genes that are downstream of FSH receptor activation and involved in the replication and endocrine activity of granulosa cells in the absence of *Smad3* (Fig. 4). *Cyp19a1* (a marker of differentiation) and *Ccnd2* (a marker of cell division) both have lower expression levels in *Smad3*-deficient granulosa cells than in WT cells, which is consistent with reduced responsiveness to gonadotropins.

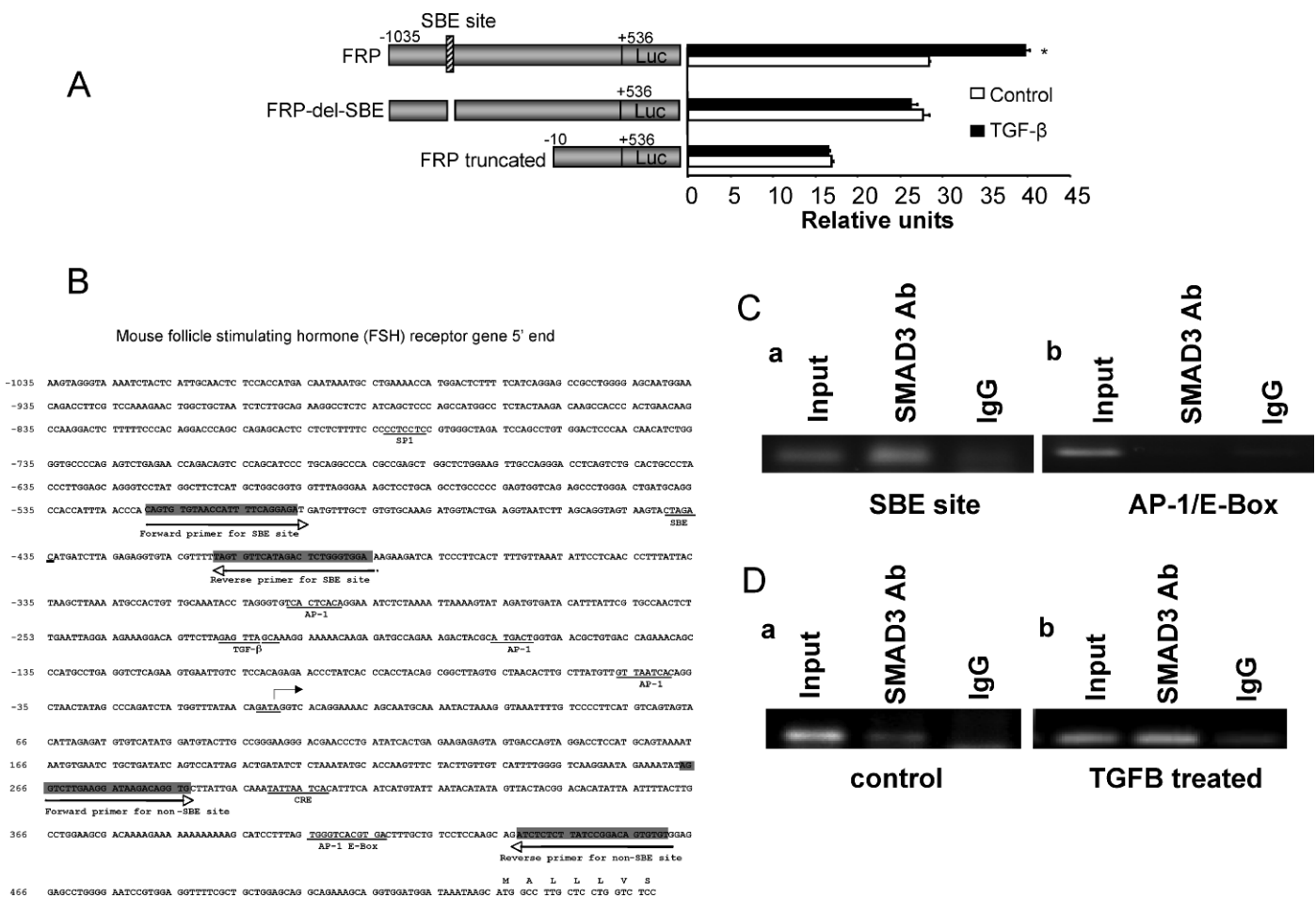


FIG. 6. *Fshr* promoter contains a SMAD-responsive element. **A**) Promoter activity of *Fshr* is increased when treated with TGFβ in the presence of a functional SBE site (FRP -440 bp). ($P < 0.05$ compared with control). *, Different from control. Constructs that are truncated (FRP truncated) or have the SBE site deleted (FRP-del-SBE) do not have increased luciferase (Luc) activity in response to TGFβ treatment. Luciferase activity is reported as relative units of fold increase over promoterless luciferase construct (PGL3-basic). Site numbers are designated as the distance from the transcription start site. Experiments were repeated three times. **B**) Map of the 5' upstream region of *Fshr*. The SBE is bolded at -440 bp. Forward and reverse primers for the ChIP assay are also labeled. Other sites of putative transcription elements are labeled (-35 bp). SMAD3 binding was not noted at any of these sites (data not shown). **C**) ChIP assay demonstrating SMAD3 binding to *Fshr* promoter. Wild-type granulosa cells were cultured with FSH for 48 h, followed by cross-linking, sonication, and immunoprecipitation with SMAD3 antibody (Ab) or IgG. Polymerase chain reactions were performed with a set of primers flanking the SBE site (a) and with another set of primers flanking the AP-1/E-Box site (b). Input is the positive control, and IgG is the negative control. **D**) ChIP assay of control and TGFβ-treated cells. Wild-type cells were serum starved and cultured without (a) and with (b) TGFβ for 24 h. The PCR was performed with the primers for the SBE site. Input and IgG are positive and negative controls, respectively.

However, these two genes may also be under direct regulation by *Smad3* [31]. Of note, FSH serum levels are higher in *Smad3*-deficient mice than in WT mice [13], which is also consistent with reduced responsiveness to FSH at the level of the ovary.

Together, the results of the in vivo and in vitro studies lead to the conclusion that the delay in follicle progression in the *Smad3*-deficient mouse ovary results from reduced ability of the follicle to respond to FSH stimulation. This reduced ability correlates with reduced expression of *Fshr* in the granulosa cells of the *Smad3*-deficient ovaries (Fig. 4). The add-back experiments shown in Figure 5 further substantiate this conclusion. When *Smad3* expression is restored in granulosa cells, they regain their ability to respond to FSH treatment with increased *Fshr* expression.

Our findings of reduced FSH receptor expression in *Smad3*-deficient ovaries (Fig. 4) are in contrast to those by Tomic et al. [13, 14] and by Looyenga and Hammer [36], who reported that there was none or only a modest decrease in *Fshr* expression as determined by real-time PCR. The apparent discrepancy in this

important observation can be explained by differences in experimental protocol that obscured the discovery of reduced *Fshr* expression. In both of these studies [14, 36], whole-ovarian lysates from sexually mature WT ovaries were compared with similarly aged *Smad3*-deficient ovaries, which we have shown (Fig. 1) are smaller than WT ovaries and have few, if any, corpora lutea.

Corpora lutea make up a large portion of ovarian volume and have a lower expression of FSH receptors than growing antral follicles [37]. Comparing cycling whole ovaries with noncycling ovaries introduces the possibility that *Fshr* expression as a percentage of all the mRNA in an ovary is less than the *Fshr* expression in the same ovary at diestrus or even before the first ovulation. Comparing relative RNA expression from a whole organ depends highly on the cellular composition and stages of maturation making up that organ. The difference in cycling WT versus noncycling *Smad3*-deficient ovaries is further emphasized and confirmed by examining the LH receptor expression in the two different ovary lysates from the study by Looyenga and Hammer [36].

In the WT ovaries, LH receptor is expressed at very high levels, yet LH receptor expression was almost nonexistent in the *Smad3* KO lysates, consistent with the observation that there were fewer corpora lutea in the KO ovaries compared with the WT ovaries in that experiment. Our design bypasses the issue of comparing whole-ovary lysates of cycling animals with those of noncycling animals. We compared matched prepubertal sibling pair ovaries, as well as freshly isolated granulosa cells and cultured cells. Thus, in three different systems the basal expression of *Fshr* in granulosa cells is reduced in the absence of *Smad3* expression. Our functional studies also confirm these conclusions because FSH-stimulated *in vivo* cell division, follicle growth, and *in vitro* cell division were all impaired in *Smad3*-deficient mice (Figs. 3 and 4). Furthermore, add-back of SMAD3 restores FSH responsiveness and FSH receptor expression (Fig. 5).

The *Smad3*-deficient mouse has an embryonic lethal phenotype, so its specific ovarian effects are unknown. SMAD2 and SMAD3 are very highly homologous molecules and share many functions [11, 38]. Thus, some of the functions of SMAD3 may be compensated for by SMAD2. However, there are differences in the two molecules. SMAD3 is able to bind DNA on its own, but SMAD2 must interact with other cofactors. SMAD2 and SMAD3 have different affinities for cofactors and can interact with different factors in different cell types [38]. SMAD3 and SMAD2 are both expressed in preantral follicles, and the expression of both declines in antral and larger follicles. However, only SMAD2 expression returns in the corpus luteum [12]. Because of this expression pattern, the effects of SMAD3 deletion must be predominantly in the smaller growing follicles. A recent study [39] has compared the roles of SMAD3 and SMAD2 in ovarian function by using conditional KOs with a different *Smad3* deletion construct from that in this colony. The study demonstrated redundancy in some roles of *Smad2* and *Smad3* in ovarian function, particularly in cumulus expansion. However, *Fshr* expression or function was not evaluated, so this effect cannot yet be compared in these models. Differences in the constructs used and the possibility of residual production of a small amount of SMAD3 protein with the exon 2 deletion construct also make direct comparison of preantral effects of *Smad3* difficult. Further studies will be necessary to discern the causes of phenotypic differences in the two constructs used to create *Smad3*-deficient mice.

Our studies demonstrate that the ability of FSH to upregulate its own receptor is diminished in the absence of *Smad3*. This may be a critical process that is disrupted in the *Smad3*-deficient ovary and one that has been overlooked in previous studies. The restoration of functional SMAD3 to the granulosa cells allowed the expression of *Fshr* to recover to normal levels and restored the ability of FSH treatment to upregulate its receptor. Forskolin alone was not sufficient to increase *Fshr* in the *Smad3*-deficient cells (Fig. 4), although it did in the WT cells. Therefore, reduced cAMP levels do not appear to be solely responsible for the reduced expression of *Fshr* in the absence of SMAD3.

Both activin and TGF β , which signal through both SMAD2 and SMAD3, increase mRNA expression for *Fshr* in cultured granulosa cells [5, 6]. In our studies, activin A did not increase FSH-stimulated *Fshr* expression in the absence of *Smad3*, although it did in the WT cells. Further studies are necessary to clarify the levels of regulation and the role of signaling cross talk in determining *Fshr* regulation and downstream function. However, SMAD3 can bind to and increase the activity of the *Fshr* promoter. An increase in *Fshr* expression stimulated by TGF β (or a family member) in early follicles could be one

mechanism by which *Smad3* function enhances early follicle development.

The ability of a preantral follicle to respond to FSH treatment with growth and differentiation affects its ability to eventually become a preovulatory follicle. Factors that affect the responsiveness of follicles to FSH can affect fecundity and ultimate fertility. We have demonstrated that a signal transduction protein for a major growth factor family has a key role in *Fshr* expression *in vitro* and *in vivo*. Genes regulating FSH receptor activity may be of great functional importance. Infertility in women is not generally an all-or-nothing issue but is rather more appropriately described as subfertility. *Smad3* deficiency does not turn off the FSH receptor, but it does reduce the ability of the granulosa cell to respond to gonadotropins. Thus, alterations in ovarian responsiveness and the dynamics of follicular development that are frequently found in the treatment of infertility may be caused, in part, by alterations in SMAD3 signaling. Normal dynamics of early follicle growth may be as important to fertility as the far more studied dynamics of later antral and preovulatory follicle growth and development. Although difficult to perform, studies of modulating influences on gamete production may produce rewards in our future understanding of the causes of human subfertility.

ACKNOWLEDGMENTS

We acknowledge the excellent technical assistance of Pam Gigliotti and the technical advice from Dr. Zhibing Zhang, Dr. Chen Chen, and Dr. Tony Zeleznik. We thank Dr. Jerome F. Strauss III for thoughtful conversations and editorial assistance.

REFERENCES

1. McGee EA, Hsueh AJ. Initial and cyclic recruitment of ovarian follicles. *Endocr Rev* 2000; 21:200–214.
2. McGee EA, Perlas E, LaPolt PS, Tsafiriri A, Hsueh AJ. Follicle-stimulating hormone enhances the development of preantral follicles in juvenile rats. *Biol Reprod* 1997; 57:990–998.
3. Adashi EY. With a little help from my friends: the evolving story of intraovarian regulation. *Endocrinology* 1995; 136:4161–4162.
4. Knight PG, Glistler C. TGF- β superfamily members and ovarian follicle development. *Reproduction* 2006; 132:191–206.
5. Inoue K, Nakamura K, Abe K, Hirakawa T, Tsuchiya M, Oomori Y, Matsuda H, Miyamoto K, Minegishi T. Mechanisms of action of transforming growth factor beta on the expression of follicle-stimulating hormone receptor messenger ribonucleic acid levels in rat granulosa cells. *Biol Reprod* 2003; 69:1238–1244.
6. Minegishi T, Kishi H, Tano M, Kameda T, Hirakawa T, Miyamoto K. Control of FSH receptor mRNA expression in rat granulosa cells by 3',5'-cyclic adenosine monophosphate, activin, and follistatin. *Mol Cell Endocrinol* 1999; 149:71–77.
7. Hayashi M, McGee EA, Min G, Klein C, Rose UM, van Duin M, Hsueh AJ. Recombinant growth differentiation factor-9 (GDF-9) enhances growth and differentiation of cultured early ovarian follicles. *Endocrinology* 1999; 140:1236–1244.
8. McGee EA, Smith R, Spears N, Nachtigal MW, Ingraham H, Hsueh AJ. Mullerian inhibitory substance induces growth of rat preantral ovarian follicles. *Biol Reprod* 2001; 64:293–298.
9. Thomas FH, Armstrong DG, Telfer EE. Activin promotes oocyte development in ovine preantral follicles *in vitro*. *Reprod Biol Endocrinol* 2003; 1:76–83.
10. Thomas FH, Ethier JF, Shimasaki S, Vanderhyden BC. Follicle-stimulating hormone regulates oocyte growth by modulation of expression of oocyte and granulosa cell factors. *Endocrinology* 2005; 146:941–949.
11. Wrana JL. Crossing Smads. *Sci STKE* 2000; 2000:eRE1.
12. Xu J, Oakley J, McGee EA. Stage-specific expression of Smad2 and Smad3 during folliculogenesis. *Biol Reprod* 2002; 66:1571–1578.
13. Tomic D, Brodie SG, Deng C, Hickey RJ, Babus JK, Malkas LH, Flaws JA. Smad 3 may regulate follicular growth in the mouse ovary. *Biol Reprod* 2002; 66:917–923.
14. Tomic D, Miller KP, Kenny HA, Woodruff TK, Hoyer P, Flaws JA.

- Ovarian follicle development requires Smad3. *Mol Endocrinol* 2004; 18: 2224–2240.
15. Yang X, Letterio JJ, Lechleider RJ, Chen L, Hayman R, Gu H, Roberts AB, Deng C. Targeted disruption of SMAD3 results in impaired mucosal immunity and diminished T cell responsiveness to TGF- β . *Embryo J* 1999; 18:1280–1291.
 16. Roberts AB, Russo A, Felici A, Flanders KC. Smad3: a key player in pathogenetic mechanisms dependent on TGF- β . *Ann N Y Acad Sci* 2003; 995:1–10.
 17. Weinstein M, Yang X, Deng C. Functions of mammalian Smad genes as revealed by targeted gene disruption in mice. *Cytokine Growth Factor Rev* 2000; 11:49–58.
 18. Nothnick WB, Soloway P, Curry TE Jr. Assessment of the role of tissue inhibitor of metalloproteinase-1 (TIMP-1) during the periovulatory period in female mice lacking a functional TIMP-1 gene. *Biol Reprod* 1997; 56: 1181–1188.
 19. McGee EA, Chun SY, Lai S, He Y, Hsueh AJ. Keratinocyte growth factor promotes the survival, growth, and differentiation of preantral ovarian follicles. *Fertil Steril* 1999; 71:732–738.
 20. McGee E, Spears N, Minami S, Hsu SY, Chun SY, Billig H, Hsueh AJ. Preantral ovarian follicles in serum-free culture: suppression of apoptosis after activation of the cyclic guanosine 3',5'-monophosphate pathway and stimulation of growth and differentiation by follicle-stimulating hormone. *Endocrinology* 1997; 138:2417–2424.
 21. Campbell KL. Ovarian granulosa cells isolated with EGTA and hypertonic sucrose: cellular integrity and function. *Biol Reprod* 1979; 21:773–786.
 22. Livak KJ, Schmittgen TD. Analysis of relative gene expression data using real-time quantitative PCR and the 2 $^{-\Delta\Delta C_T}$ method. *Methods* 2001; 25:402–408.
 23. Jung M, Ramankulov A, Roigas J, Johannsen M, Ringsdorf M, Kristiansen G, Jung K. In search of suitable reference genes for gene expression studies of human renal cell carcinoma by real-time PCR. *BMC Mol Biol* 2007; 8:e47.
 24. Peluso JJ, Pappalardo A. Progesterone regulates granulosa cell viability through a protein kinase G-dependent mechanism that may involve 14-3-3 σ . *Biol Reprod* 2004; 71:1870–1878.
 25. Geles KG, Freiman RN, Liu WL, Zheng S, Voronina E, Tjian R. Cell-type-selective induction of c-jun by TAF4b directs ovarian-specific transcription networks. *Proc Natl Acad Sci U S A* 2006; 103:2594–2599.
 26. Stein LS, Stoica G, Tilley R, Burghardt RC. Rat ovarian granulosa cell culture: a model system for the study of cell-cell communication during multistep transformation. *Cancer Res* 1991; 51:696–706.
 27. Chipuk JE, Cornelius SC, Pultz NJ, Jorgensen JS, Bonham MJ, Kim SJ, Danielpour D. The androgen receptor represses transforming growth factor- β signaling through interaction with Smad3. *J Biol Chem* 2002; 277:1240–1248.
 28. Sommers JP, DeLoia J, Zeleznik AJ. Adenovirus-directed expression of a nonphosphorylated mutant of CREB (cAMP response element binding protein) adversely affects the survival, but not the differentiation, of rat granulosa cells. *Mol Endocrinol* 1999; 13:1364–1372.
 29. Murray A, Spears N. Follicular development in vitro. *Semin Reprod Med* 2000; 18:109–122.
 30. Gaytan F, Morales C, Bellido C, Aguilar E, Sanchez-Criado JE. Proliferative activity in the different ovarian compartments in cycling rats estimated by the 5-bromodeoxyuridine technique. *Biol Reprod* 1996; 54: 1356–1365.
 31. Park Y, Maizels ET, Feiger ZJ, Alam H, Peters CA, Woodruff TK, Unterman TG, Lee EJ, Jameson JL, Hunzicker-Dunn M. Induction of cyclin D2 in rat granulosa cells requires FSH-dependent relief from FOXO1 repression coupled with positive signals from Smad. *J Biol Chem* 2005; 280:9135–9148.
 32. Zawal L, Dai J, Buckhaults P, Zhou S, Kinzler K, Vogelstein B, Kern SE. Human Smad3 and Smad4 are sequence-specific transcription activators. *Mol Cell* 1988; 1:611–617.
 33. Denissova N, Pouponnot C, Long J, He D, Liu F. Transforming growth factor β -inducible independent binding of SMAD to the Smad7 promoter. *Proc Natl Acad Sci U S A* 2000; 97:6397–6402.
 34. Wu Y, Zhang X, Salmon M, Lin X, Zehner ZE. TGF β 1 regulation of vimentin gene expression during differentiation of the C2C12 skeletal myogenic cell line requires Smads, Ap-1 and Sp1 family members. *Biochim Biophys Acta* 2007; 1773:427–439.
 35. Levallet J, Koskimies P, Rahman N, Huhtaniemi I. The promoter of murine follicle-stimulating hormone receptor: functional characterization and regulation by transcription factor steroidogenic factor 1. *Mol Endocrinol* 2001; 15:80–92.
 36. Looyenga BD, Hammer GD. Genetic removal of Smad3 from inhibin-null mice attenuates tumor progression by uncoupling extracellular mitogenic signals from the cell cycle machinery. *Mol Endocrinol* 2007; 10:2440–2457.
 37. Liu J, Aronow B, Witte DP, Pope WF, La Barbera A. Cyclic and maturation-dependent regulation of follicle-stimulating hormone receptor and luteinizing hormone receptor messenger ribonucleic acid expression in the porcine ovary. *Biol Reprod* 1998; 58:648–658.
 38. Massague J, Gomis RR. The logic of TGF β signaling. *FEBS Lett* 2006; 580:2811–2820.
 39. Li Q, Pangas SA, Jorgez CJ, Graff JM, Weinstein M, Matzuk MM. Redundant roles of SMAD2 and SMAD3 in ovarian granulosa cells in vivo. *Mol Cell Biol* 2008; 28:7001–7011.